# Hsp42 is required for sequestration of protein aggregates into deposition sites in *Saccharomyces cerevisiae*

Sebastian Specht, Stephanie B.M. Miller, Axel Mogk, and Bernd Bukau

Zentrum für Molekulare Biologie der Universität Heidelberg, Deutsches Krebsforschungszentrum, DKFZ–ZMBH Allianz, Im Neuenheimer Feld 282, Heidelberg 69120, Germany

The aggregation of proteins inside cells is an organized process with cytoprotective function. In *Saccharomyces cerevisiae*, aggregating proteins are spatially sequestered to either juxtanuclear or peripheral sites, which target distinct quality control pathways for refolding and degradation. The cellular machinery driving the sequestration of misfolded proteins to these sites is unknown. In this paper, we show that one of the two small heat shock proteins of yeast, Hsp42, is essential for the formation of peripheral aggregates during physiological heat stress. Hsp42 preferentially localizes to peripheral aggregates but is largely absent from juxtanuclear aggregates, which still form in hsp42Δ cells. Transferring the amino-terminal domain of Hsp42 to Hsp26, which does not participate in aggregate sorting, enables Hsp26 to replace Hsp42 function. Our data suggest that Hsp42 acts via its amino-terminal domain to coaggregate with misfolded proteins and perhaps link such complexes to further sorting factors.

## Introduction

Perturbation of protein homeostasis by various forms of stress such as exposure to heat poses a major threat to cells. The primary response of all cells to such perturbation is the refolding of misfolded proteins by molecular chaperones or their elimination by proteolysis. Although this quality control system normally adapts to the severity of protein damage through the induction of stress responses (Morimoto, 2008), high levels or continuous production of a single species of misfolded proteins exceeding its capacity ultimately results in the generation of protein aggregates. Protein aggregation has multiple and even opposing consequences for cell physiology. On the one hand, aggregation is associated with aging, pathophysiological states, and toxicity of cells, e.g., through the trapping of other proteins and poisoning of cellular processes. On the other hand, aggregation protects protein homeostasis by actively sequestering aggregation-prone proteins, which may counteract cell toxicity and facilitate subsequent quality control activities, such as the recruitment of chaperones and proteases.

Recent evidence suggests that protein aggregation is a much more organized process in vivo than previously recognized (Kaganovich et al., 2008). Aggregated proteins within cells, from bacteria to humans, are directed to specific sites, although the specific localizations of deposition sites and the mechanisms of aggregate sorting differ between organisms. In the bacterium *Escherichia coli*, protein aggregates localize to cell poles (Lindner et al., 2008; Rokney et al., 2009; Winkler et al., 2010) by a passive mechanism that relies on aggregate-excluding effects of the centrally located chromosome (Winkler et al., 2010). In mammalian cells, several forms of aggregates exist. Aggresomes are perinuclear protein aggregates located at the microtubule-organizing center (Johnston et al., 1998). Misfolded proteins are actively sequestered in the aggresome by a process involving dynein and histone deacetylase 6 (HDAC6)–dependent retrograde transport along microtubules (Johnston et al., 1998; García-Mata et al., 1999; Rujano et al., 2006). Perinuclear deposition sites that form upon inhibition of the proteasome have also been described (Lelouard et al., 2002; Szeto et al., 2006; Kaganovich et al., 2008), although the relation of

Correspondence to Bernd Bukau: bukau@zmbh.uni-heidelberg.de; or Axel Mogk: a.mogk@zmbh.uni-heidelberg.de

Abbreviations used in this paper: CTE, C-terminal extension; FLIP, fluorescence loss in photobleaching; IPOD, insoluble protein deposit; LatA, latrunculin A; mCFP, monomeric CFP; mCitrine, monomeric Citrine; NTD, N-terminal domain; sHSP, small heat shock protein; VHL, von Hippel–Lindau; WT, wild type; YPD, yeast peptone dextrose.



The Rockefeller University Press $30.00
J. Cell Biol. Vol. 195 No. 4 617–629
www.jcb.org/cgi/doi/10.1083/jcb.201106037

these to aggresomes is not well understood. Amyloidogenic proteins are sequestered in mammalian cells to sites that differ from the perinuclear inclusions (Kaganovich et al., 2008). In the yeast *Saccharomyces cerevisiae*, two distinct compartments for accumulating misfolded proteins upon proteasomal inhibition were described, the juxtanuclear quality control compartment (JUNQ) and the perivacuolar insoluble protein deposit (IPOD; Kaganovich et al., 2008). The JUNQ compartment accumulates misfolded proteins that retain relatively high mobility and are ubiquitinated and likely represent substrates for proteasomal degradation. In contrast, the IPOD compartment harbors terminally aggregated immobile proteins, including amyloidogenic proteins such as the yeast prion [RNQ]. The formation of both deposition sites is thought to rely on a functional microtubule cytoskeleton (Kaganovich et al., 2008). However, the identity of the cellular machinery that mediates the sorting and sequestration of misfolded proteins to the JUNQ and IPOD compartments remains largely elusive.

Here, we have studied the sequestration of aggregating proteins under physiological stress conditions in *S. cerevisiae* by using fluorescent reporter proteins. We performed a detailed quantitative time-resolved analysis of the aggregation process in thermally stressed cells, leading to a refined description of the initial stages and subsequent intracellular organization of protein aggregation. We further demonstrate that the small heat shock protein (sHSP) Hsp42, via its extended N-terminal domain (NTD), associates preferentially with peripheral aggregates and is essential for the targeting of misfolded proteins to these sites. The other sHSP, Hsp26, associates with both peripheral and perinuclear aggregates under severe heat shock conditions exclusively. Our findings indicate novel and distinct roles for the sHSP class of chaperones in the cellular organization and sorting of protein aggregates.

## Results

### Fluorescent reporters for monitoring protein aggregation

We analyzed the formation of protein aggregates in yeast cells by monitoring the behavior of two fluorescent reporter proteins, which are prone to misfolding for distinct reasons, and a reporter, which associates with endogenous protein aggregates without becoming aggregated itself. First, we used the previously characterized N-terminal fusion of mCherry and von Hippel–Lindau (VHL) tumor suppressor protein, which was produced to high levels in the presence of galactose from a 2-µm plasmid (Kaganovich et al., 2008). Unassembled VHL in the absence of its cofactor elongin BC is prone to misfolding at 37°C and is rapidly degraded (McClellan et al., 2005). Upon inhibition of the proteasome, mCherry-VHL aggregates and partitions to both JUNQ and IPOD compartments (Kaganovich et al., 2008). Second, we constructed an N-terminal fusion of monomeric Citrine (mCitrine) with thermolabile *Photinus pyralis* luciferase, which serves as a marker for protein misfolding under thermal stress (Schröder et al., 1993; Winkler et al., 2010). The fusion gene was integrated into the chromosome under control of the constitutive *ACT1* promoter, yielding moderate cellular levels of mCitrine-luciferase (unpublished data). Third, we C-terminally fused the chromosomal copy of the Hsp104 disaggregase to monomeric CFP (mCFP). The fusion protein was fully active in protein disaggregation in vivo (Fig. S1) and, because of its property of associating specifically with aggregated proteins, served as a marker for cellular aggregates of endogenous yeast proteins (Kaganovich et al., 2008; Liu et al., 2010).

We analyzed the localization of the three fusion proteins in cells grown at 30°C and at various time points after a shift to 37°C in the presence of the proteasome inhibitor MG132 (Fig. 1 A). This treatment represents a mild heat shock condition and permits us to monitor the fate of protein aggregates over time. All recorded pictures represent maximal projections of individual sections of yeast cells, allowing for accurate determination of numbers of stress-induced reporter foci. At 30°C, mCherry-VHL and mCitrine-luciferase displayed a homogeneous cytosolic distribution, whereas Hsp104-mCFP was enriched in the nucleus (Fig. 1 A). Incubation of the cells at 37°C triggered foci formation, reaching a maximal number of three or more cytosolic mCherry-VHL and Hsp104-mCFP foci/cell in ∼70% of cells after a 30-min incubation (Fig. 1 B), which is in accordance with published data (Kaganovich et al., 2008). In the case of mCitrine-luciferase, slightly fewer foci/cell were detectable (Fig. 1 B). After prolonged incubation at 37°C for 180 min, the number of fluorescent foci per cell was reduced, indicating aggregate clearance and sorting; longer incubation did not result in further reduction of the number of foci per cell (unpublished data). After 180 min, in ∼50% of the cells, mCherry-VHL accumulated in one juxtanuclear aggregate and one aggregate distant from the nucleus (hereafter referred to as peripheral). The remaining cells exhibited single or multiple juxtanuclear or peripheral aggregates or a combination of both (Fig. 1 B). Similar to mCherry-VHL, after 180 min, ∼40–45% of the cells accumulated Hsp104-mCFP and mCitrine-luciferase in one juxtanuclear and one peripheral aggregate, whereas the remaining cells mainly possessed only a single juxtanuclear aggregate. In short, comparable numbers and cellular locations of aggregates were detectable, irrespective of the investigated aggregation reporter. The simultaneous expression of mCherry-VHL and mCitrine-luciferase also revealed a high degree of colocalization upon stress treatment (37°C, MG132; Fig. 1 C), indicating that structurally unrelated substrates share the same fate and are recruited to the same compartments. The reduced overall number of mCitrine-luciferase aggregates as compared with mCherry-VHL and Hsp104-mCFP aggregates is likely a result of lower expression levels and only partial misfolding of the thermolabile reporter at 37°C. Incubation at 37°C without the addition of MG132 yielded comparable numbers and localizations of Hsp104-mCFP foci, although the intensities of the foci were slightly reduced (unpublished data). Therefore, the presence of MG132 increases the severity of the applied stress condition but does not affect aggregate formation and sorting in a fundamental way.

Collectively, our observations reveal that we can distinguish juxtanuclear and more peripheral protein aggregates, but there is more heterogeneity with respect to the number/cell and intracellular localization of the aggregates than previously described (Kaganovich et al., 2008). Hereafter, therefore, we will distinguish between juxtanuclear and peripheral aggregates.

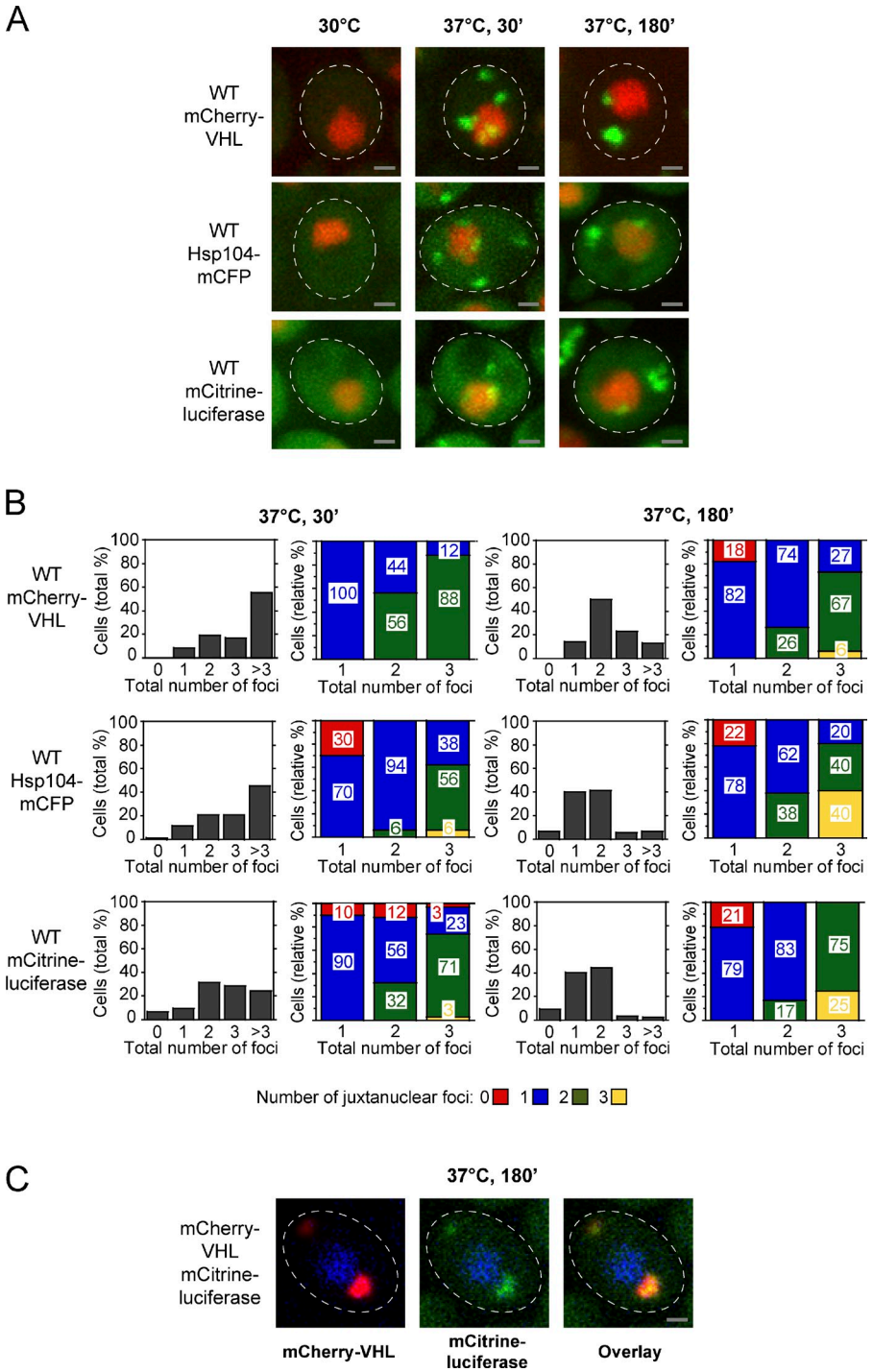


Figure 1. **Spatiotemporal organization of protein aggregates in yeast cells.** (A) Time-dependent changes in the localization of mCherry-VHL, Hsp104-mCFP, and mCitrine-luciferase (all green) in WT cells grown at 30°C and after a shift to 37°C for 30 and 180 min. MG132 was added before the temperature shift. Nuclei were visualized by coexpressing HTB1-cerulean or HTB1-mCherry (red). (B) Number (shaded bars) and localization (colored bars) of mCherry-VHL, Hsp104-mCFP, and mCitrine-luciferase aggregates in WT cells after incubation at 37°C for 30 and 180 min. The total number of foci per cell (juxtanuclear and peripheral) is depicted in all diagrams on the x axis. Quantifications are based on the analysis of 50–120 cells and are representatives of multiple experimental repeats. (C) Different substrates are sorted to the same compartments. mCherry-VHL (red) and mCitrine-luciferase (green) were coexpressed in WT cells. Protein localizations were determined after a temperature shift to 37°C for 180 min, revealing colocalization of mCherry-VHL and mCitrine-luciferase. Nuclei were visualized by coexpressing HTB1-cerulean (blue). The dashed lines indicate the border of respective yeast cells. Bars, 1 µm.



## Hsp42 affects the organization of protein aggregates

Little is known about the factors that target aggregation-prone proteins to specific sites within the cell. We considered the sHSPs as candidates for a role in this process because these chaperones efficiently coaggregate with misfolded proteins, thereby altering the properties of protein aggregates and facilitating disaggregation by chaperones (Giese and Vierling, 2002; Mogk et al., 2003; Cashikar et al., 2005; Haslbeck et al., 2005b; Ratajczak et al., 2009). We tested whether either of the two yeast sHSPs, Hsp26 and Hsp42, had a role in the sequestration process by comparing the localization of mCherry-VHL and Hsp104-mCFP in hsp26Δ and hsp42Δ mutant cells (Fig. 2). The lack of Hsp26 in hsp26Δ cells had only a minor influence on stress-induced formation of mCherry-VHL and Hsp104-mCFP aggregates. Number and localization of respective aggregates were largely similar to those observed for wild-type (WT) cells at both time points (Fig. 2, A–D).

In sharp contrast, in the vast majority (>75%) of hsp42Δ cells, we detected only one juxtanuclear mCherry-VHL aggregate/cell of higher fluorescence intensity, whereas peripheral aggregates were absent at shorter (30 min) and longer (180 min)

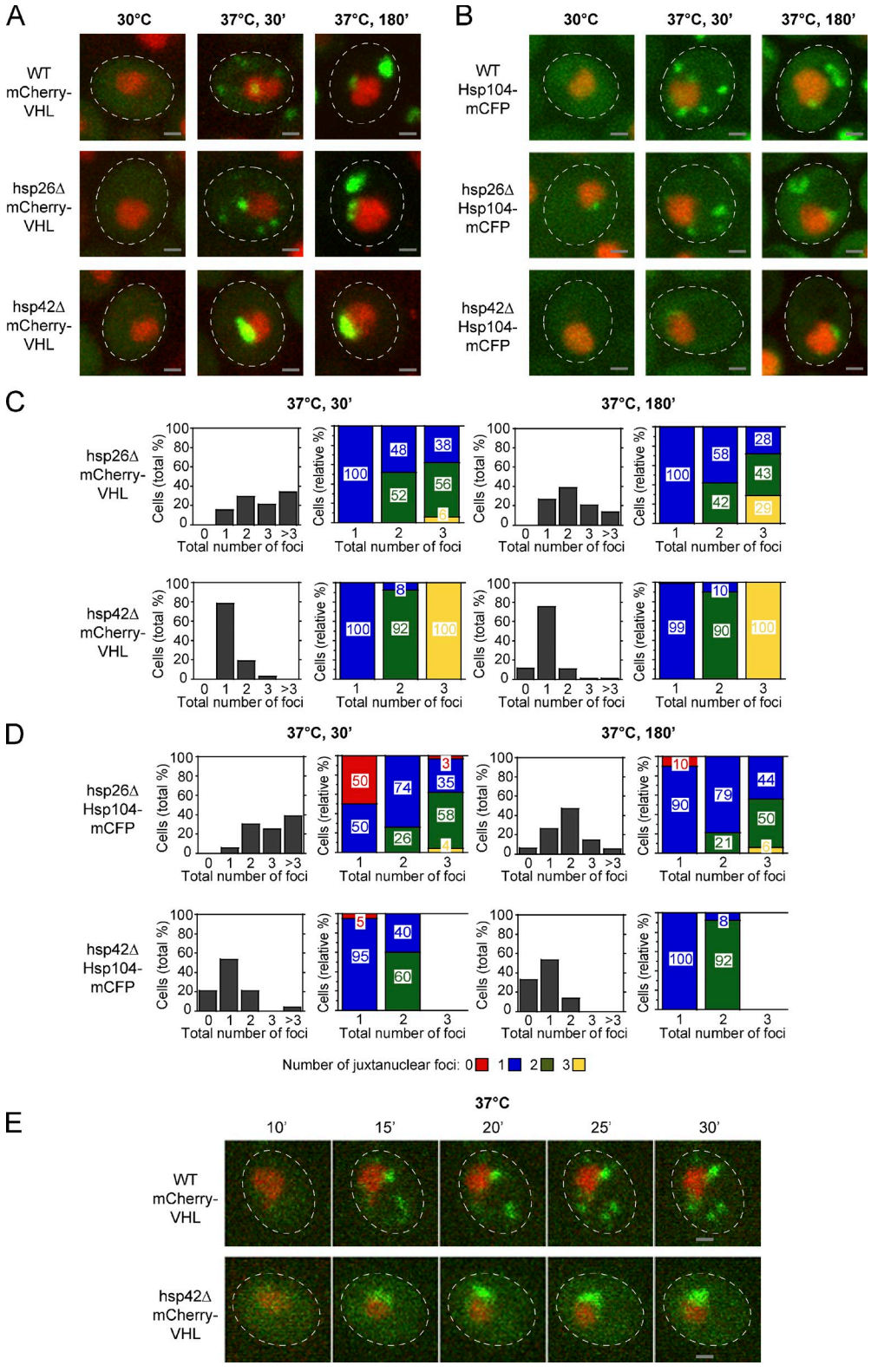


Figure 2. **Hsp42 is essential for the targeting of misfolded proteins to peripheral aggregates.** (A and B) Time-dependent changes in the localization of mCherry-VHL (A) and Hsp104-mCFP (B; both green) at 30°C and after a shift to 37°C for 30 and 180 min in the isogenic WT, hsp26Δ, and hsp42Δ strains. MG132 was added before the temperature shift. Nuclei were visualized by coexpressing HTB1-cerulean or HTB1-mCherry (red). (C and D) Number (shaded bars) and localization (colored bars) of mCherry-VHL (C) and Hsp104-mCFP (D) aggregates in hsp26Δ and hsp42Δ cells after incubation at 37°C for 30 and 180 min. MG132 was added before the temperature shift. The total number of foci per cell is depicted on the x axis in all diagrams. Quantifications are based on the analysis of 70–90 cells and are representatives of at least two experimental repeats. (E) In hsp42Δ cells, mCherry-VHL foci form exclusively at the nucleus. Time-lapse microscopy pictures of single WT and hsp42Δ cells expressing mCherry-VHL (green) after a shift to 37°C for the indicated time period. MG132 was added before the temperature shift. Nuclei were visualized by coexpressing HTB1-cerulean (red). The dashed lines indicate the border of respective yeast cells. Bars, 1 µm.

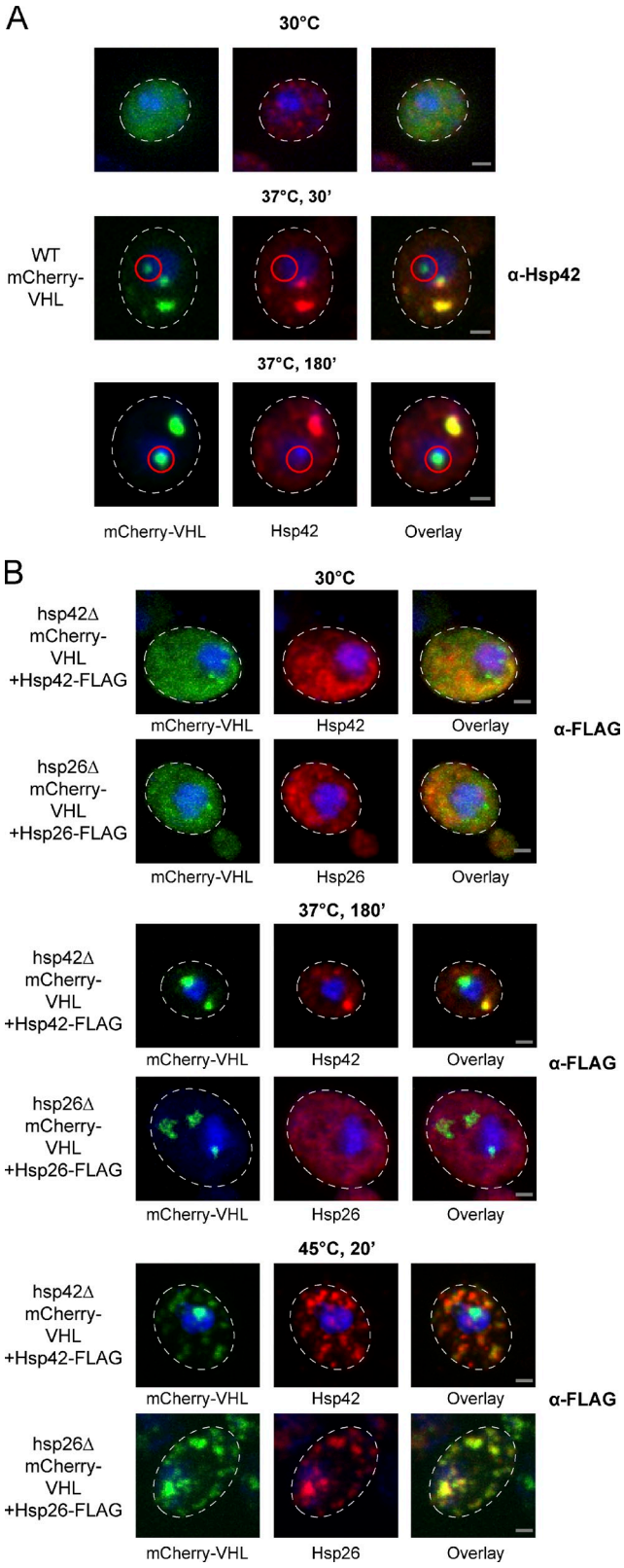


Figure 3. **Hsp42 localizes exclusively to peripheral mCherry-VHL inclusions.** (A) WT cells expressing mCherry-VHL were grown at 30°C and shifted to 37°C (+MG132). The cellular localizations of mCherry-VHL (green) and Hsp42 (red) were determined at the indicated time points. Hsp42 localization was determined by immunofluorescence using Hsp42-specific antibodies. Nuclei were visualized by coexpressing HTB1-cerulean (blue). Juxtanuclear mCherry-VHL foci that do not colocalize with Hsp42 are highlighted by red circles. (B) hsp42Δ or hsp26Δ cells coexpressing mCherry-VHL and Hsp42-FLAG or Hsp26-FLAG as indicated were grown at 30°C and shifted to 37°C (+MG132) for 180 min or to 45°C (+MG132) for 20 min. mCherry-VHL is depicted in green, and sHSP stainings using FLAG antibodies are shown in red. Nuclei were visualized by DAPI staining (blue). The dashed lines indicate the border of respective yeast cells. Bars, 1 µm.

time after stress application (Fig. 2, A–D). Similarly, aggregates of endogenous misfolded yeast proteins marked by Hsp104-mCFP mostly localized to juxtanuclear sites in hsp42Δ cells (Fig. 2, A–D), and mCitrine-luciferase aggregates localized almost exclusively to juxtanuclear sites in hsp42Δ cells upon temperature upshift to 37°C (not depicted). Single-cell time-lapse microscopy revealed that, whereas in WT cells aggregates of mCherry-VHL appeared at both juxtanuclear and peripheral sites after 15 min (Fig. 2 E), in hsp42Δ cells, mCherry-VHL aggregates only formed at juxtanuclear sites. The sorting of misfolded proteins to peripheral deposition sites therefore requires Hsp42.

## Hsp42 localizes preferentially to peripheral deposition sites

We hypothesized that the almost complete absence of peripheral aggregates in hsp42Δ cells results from a direct participation of Hsp42 in the formation of these foci. To test this hypothesis, we monitored the cellular localization of Hsp42 before and after stress treatment by immunofluorescence. At 30°C, Hsp42 exhibited a largely diffuse cytosolic staining. Temperature upshift to 37°C for 30 min (+MG132) induced the formation of large Hsp42 foci, which in most cells (90%; $n = 40$) colocalized with all mCherry-VHL aggregates except for the one (90% of cells) or two (10% of cells) juxtanuclear aggregates, which failed to stain with the Hsp42 antiserum (Fig. 3 A). Longer incubation (180 min) at 37°C yielded comparable results with respect to the selective Hsp42 staining of peripheral mCherry-VHL aggregates; in 90% of the cells ($n = 60$), juxtanuclear aggregates showed no colocalization with Hsp42 (Fig. 3 A), and only in 10% of the cells did all aggregates colocalize with Hsp42. In the latter few cases, the staining of juxtanuclear mCherry-VHL aggregates by Hsp42 antiserum is likely to be an artifact of picture acquisition, as pictures represent maximal projections of individual sections of yeast cells. In consequence, in a few cases, mCherry-VHL and Hsp42 foci, which are not directly localized at the nucleus, will be incorrectly classified as juxtanuclear aggregates.

Monitoring the localization of Hsp26, immunofluorescence of the untagged protein was not possible, as the available Hsp26 antibody proved unsuitable. As an alternative approach allowing direct comparison between the localizations of Hsp26 and Hsp42, we genetically fused a C-terminal FLAG tag to Hsp26 and Hsp42. The ORFs encoding each construct were integrated into the hsp42 locus in either hsp26Δ or hsp42Δ cells. This strategy ensured comparable expression levels of both sHSPs and enabled us to monitor localization by immunofluorescence using FLAG-specific antibodies (Fig. 3 B). Incubation of the cells at 37°C for 180 min in the presence of MG132 triggered foci formation of Hsp42-FLAG, which in the majority of the cells (70%; $n = 125$) colocalized with all mCherry-VHL

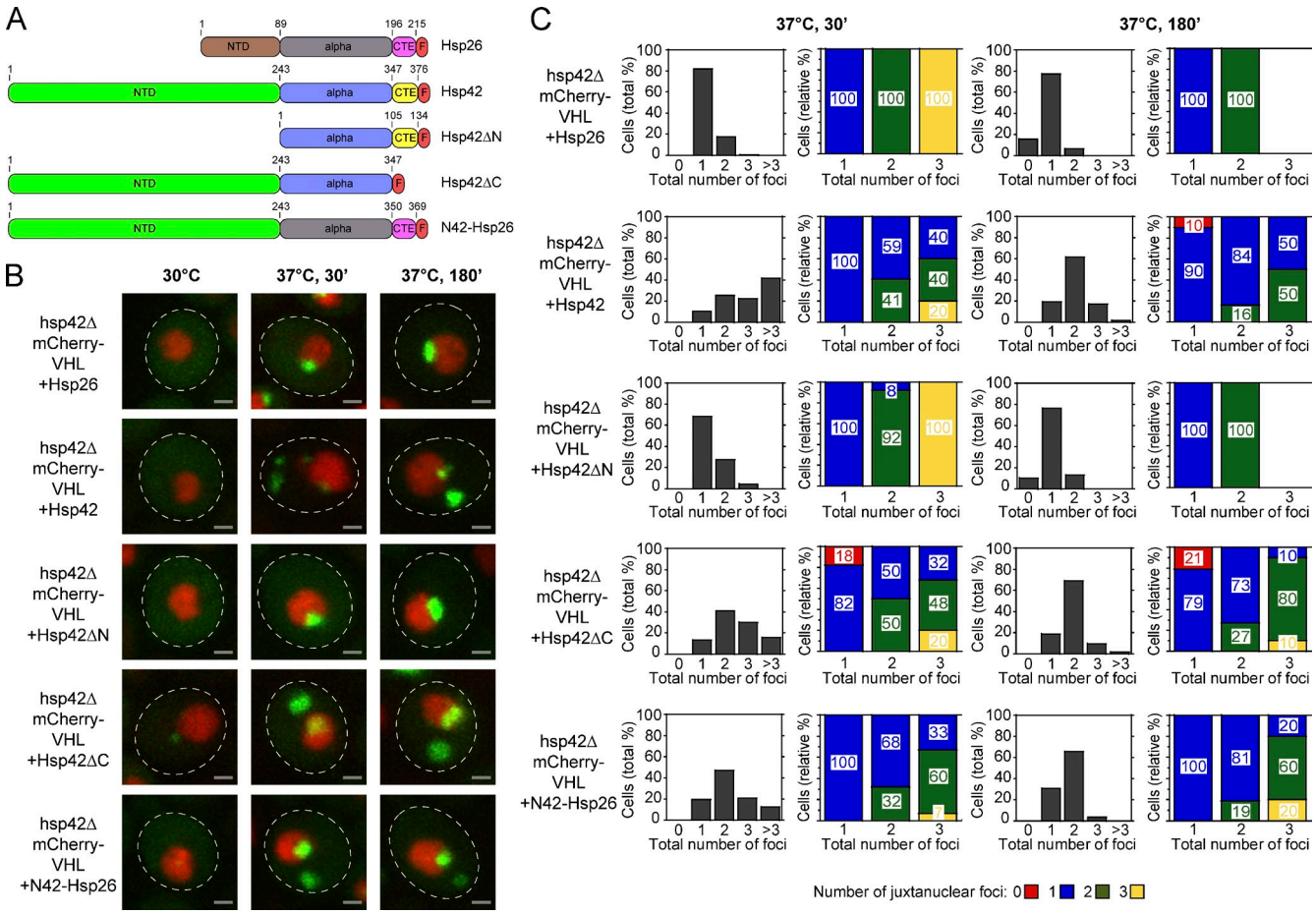


Figure 4. **The NTD of Hsp42 mediates sorting of aggregated proteins to peripheral inclusions.** (A) Domain organization of Hsp26, Hsp42, and their variants. Both sHSPs consist of an NTD, a conserved α-crystallin domain (alpha), and a CTE. All constructs were C-terminally fused to a FLAG tag (F). Domain boundaries are indicated by residue numbers. All constructs were placed under control of the native *HSP42* promoter and integrated at the Hsp42 locus in hsp42Δ cells. (B) hsp42Δ cells expressing mCherry-VHL and the indicated sHSP constructs were grown at 30°C and shifted to 37°C (+MG132). mCherry-VHL localization (green) was determined at the indicated time points. Nuclei were visualized by coexpressing HTB1-cerulean (red). The dashed lines indicate the border of respective yeast cells. Bars, 1 µm. (C) Number (shaded bars) and localization (colored bars) of mCherry-VHL inclusions in hsp42Δ cells expressing the indicated sHSP construct after incubation at 37°C for 30 and 180 min. MG132 was added before the temperature shift. The total number of foci per cell is shown on the x axis in all diagrams. Quantifications are based on the analysis of 40–130 cells and are representatives of two experimental repeats.

aggregates except the juxtanuclear aggregate (Fig. 3 B). In contrast, Hsp26-FLAG exhibited diffuse cytosolic staining before and after stress application (37°C, MG132) and hence does not coaggregate with mCherry-VHL (Fig. 3 B). Only severe heat stress treatment at 45°C caused foci formation of Hsp26-FLAG (Fig. 3 B), indicating that efficient association of this sHSP with substrates requires higher temperatures, which is in agreement with previous findings (Haslbeck et al., 1999; Franzmann et al., 2008). These severe stress conditions also led to a significant increase in the number of mCherry-VHL and Hsp42-FLAG aggregates/cell, suggesting that the sorting system for misfolded proteins becomes overwhelmed. Still, in most cells, only one juxtanuclear mCherry-VHL aggregate existed at 45°C, which failed to colocalize with Hsp42, in contrast to Hsp26, which colocalized with both forms of aggregates (Fig. 3 B).

Collectively, Hsp42 preferentially localizes to peripheral aggregates and is largely absent from the juxtanuclear aggregate, suggesting a direct role for this chaperone in the sequestration process. These findings further provide a molecular definition of both forms of aggregates based on the presence or absence of Hsp42.

## The NTD of Hsp42 is crucial for aggregate sorting

What is the molecular basis for the role of Hsp42 in controlling the sequestration of misfolded proteins to peripheral deposition sites? sHSPs are composed of an α-crystallin domain and N- and C-terminal–flanking domains, of which the NTDs exhibit the highest degree of variability in both sequence and length. *S. cerevisiae* Hsp42 has a particularly elongated NTD of 243 residues, which is therefore a prime candidate for mediating functional specificity. To investigate the role of the different Hsp42 domains, we deleted Hsp42 of its NTD (Hsp42ΔN) or C-terminal extension (CTE; Hsp42ΔC) and generated an Hsp42-Hsp26 chimera by replacing the NTD, CTE, or both domains of Hsp26 with the corresponding domain of Hsp42 (N42-Hsp26, Hsp26-C42, and NC42-Hsp26, respectively; Figs. 4 A and S2 A). In addition, all constructs harbored a C-terminal FLAG tag to

control construct expression and were integrated into the hsp42 genomic locus in hsp42Δ cells. Hsp42- and Hsp26-FLAG that were integrated into the same chromosomal site served as controls. The various sHSP constructs were expressed to similar levels (Fig. S2 D) and tested for their activity to restore the formation of peripheral mCherry-VHL aggregates.

An aggregation pattern similar to WT cells was observed upon expression of Hsp42-FLAG (Fig. 4 B). In cells expressing Hsp26-FLAG, Hsp42ΔN, or Hsp26-C42, we typically detected a single juxtanuclear aggregate and no peripheral mCherry-VHL aggregates (Figs. 4 [B and C] and S2 [B and C]). Remarkably, Hsp42ΔC and N42-Hsp26 restored the formation of peripheral fluorescent aggregates. In both backgrounds, however, the number of peripheral aggregates after a 30-min incubation at 37°C (+MG132) was slightly reduced, as compared with WT cells, suggesting that both variants exhibit only partial activity (Fig. 4, B and C). Expression of NC42-Hsp26 restored the formation of peripheral aggregates to an even higher extent (as compared with N42-Hsp26), as the number of cells carrying more than three aggregates was increased (Fig. S2, B and C). Collectively, these findings indicate that the NTD of Hsp42 plays a crucial role in allowing Hsp42 to generate peripheral aggregates.

### Localization of amyloidogenic aggregates to peripheral sites does not depend on Hsp42

In addition to some of the misfolded proteins accumulating after stress treatment, amyloidogenic proteins also are sequestered to the peripheral IPOD compartment (Kaganovich et al., 2008). Therefore, we examined whether amyloidogenic aggregates are still deposited in the peripheral IPOD compartment in hsp42Δ cells. For this purpose, we expressed in WT and hsp42Δ mutant cells the yeast prion protein RNQ1 C-terminally fused to YFP. In both strains, peripheral RNQ1-YFP foci were detectable, demonstrating that RNQ1-YFP partitioning to a peripheral site is not affected in hsp42Δ cells (Fig. 5 A). Furthermore, immunofluorescence experiments revealed that a temperature upshift to 37°C (+MG132) triggered foci formation of Hsp42, which did not overlap with RNQ-mCherry aggregates (Fig. 5 B). These findings indicate that Hsp42 acts as a marker for misfolded aggregated proteins, which are less structured than amyloid-forming prion proteins. They also imply that misfolded and amyloidogenic proteins are not targeted to the same cellular sites. In conclusion, Hsp42 is essential for the localization of amorphous, but not amyloidogenic, aggregates to peripheral sites.

### Hsp42 deficiency results in changes in dynamics and stability of juxtanuclear aggregates

What are the consequences of directing the pool of misfolded proteins exclusively to the juxtanuclear compartment in hsp42Δ cells? We compared the mobility and stability of mCherry-VHL deposited in juxtanuclear aggregates in WT and hsp42Δ cells. First, we examined the diffusion properties of misfolded proteins in the distinct compartments using fluorescence loss in photobleaching (FLIP). A small area of cytosol apart from the mCherry-VHL aggregates was repeatedly bleached with a laser pulse. The resulting loss of fluorescence in the juxtanuclear

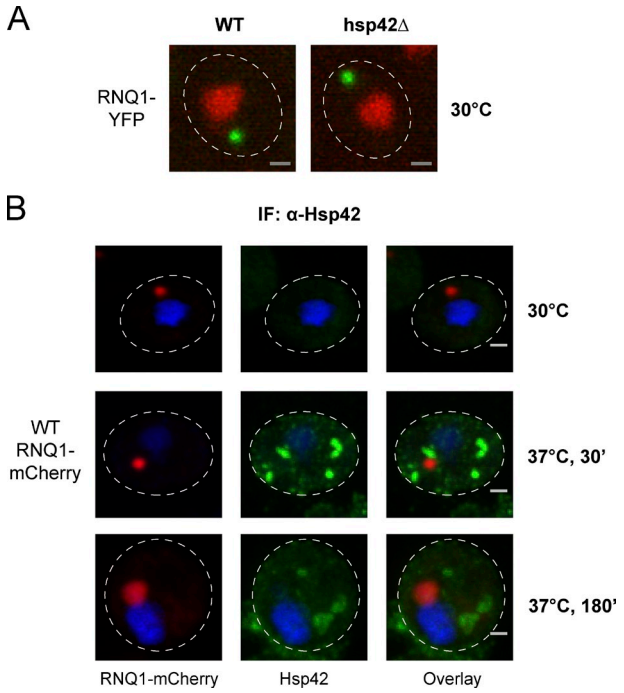


Figure 5. **Hsp42 does not affect the localization of amyloidogenic aggregates.** (A) RNQ1-YFP (green) was expressed in WT and hsp42Δ cells. Nuclei were visualized by coexpressing HTB1-mCherry (red). (B) WT cells expressing RNQ1-mCherry (green) were incubated at 30°C and shifted to 37°C for 30 min or 180 min (+MG132). The localization of Hsp42 (red) was determined by immunofluorescence (IF) using Hsp42-specific antibodies. Nuclei were visualized by DAPI staining (blue). The dashed lines indicate the border of respective yeast cells. Bars, 1 µm.

aggregate, as a function of time, provides a measure of the relative exchange rate of the aggregated mCherry-VHL with bleached cytoplasmic mCherry-VHL. Cytosolic fluorescence, which corresponds to soluble mCherry-VHL, rapidly vanished upon laser bleaching (unpublished data). In WT cells, the mCherry-VHL localized to the juxtanuclear foci displayed a slower exchange compared with cytosolic mCherry-VHL. In agreement with earlier findings (Kaganovich et al., 2008), however, this rate of loss of fluorescence was faster and more pronounced than that of molecules located in peripheral aggregates (Fig. 6 A). This indicates that the mCherry-VHL molecules present in juxtanuclear aggregates exchange more frequently with the cytosolic pool. In hsp42Δ cells, the rate of loss of fluorescence from juxtanuclear aggregates was more rapid than that of WT cells. The mCherry-VHL proteins contained within the juxtanuclear aggregate therefore display an overall increased exchange rate with the cytosolic pool in hsp42Δ cells.

Next, we studied the stability of the individual aggregate compartments by monitoring their fate upon return to physiological conditions (30°C, −MG132). After a 1-h recovery, only ∼20% of the WT cells was free of detectable mCherry-VHL aggregates, as opposed to 60% of the hsp42Δ cells (Fig. 6, B and C). After a 2-h recovery, 50% of WT cells still harbored one aggregate that predominantly (63%) exhibited a peripheral localization (Fig. 6, B and C). This implies a higher stability of peripheral aggregates as opposed to juxtanuclear aggregates. In contrast, hsp42Δ cells were almost completely devoid of

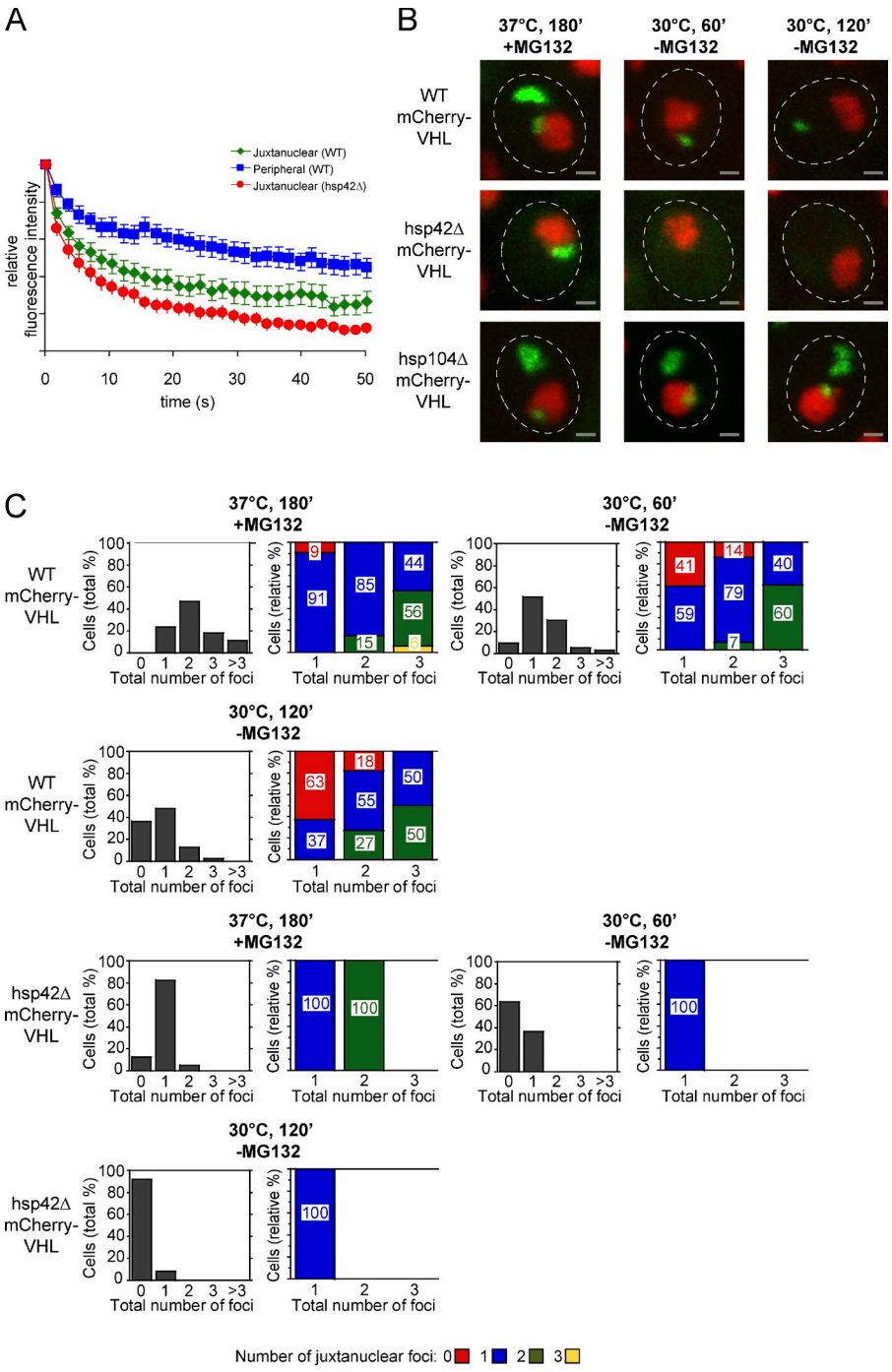


Figure 6. **The juxtanuclear aggregates of hsp42Δ cells display altered protein dynamics and stability.** (A) Juxtanuclear aggregates of hsp42Δ cells exhibit an increased exchange rate with the cytosolic mCherry-VHL pool. FLIP measurements of mCherry-VHL were performed in WT, hsp42Δ, and hsp104Δ cells after incubation at 37°C for 180 min (+MG132). Bleaching curves were calculated based on the analysis of 25 cells and the corresponding SEM. (B) mCherry-VHL aggregation foci are more rapidly resolved in the hsp42Δ strain, and their disintegration requires Hsp104-mediated protein disaggregation. WT, hsp42Δ, and hsp104Δ cells expressing mCherry-VHL (green) were grown at 30°C and shifted to 37°C for 180 min (+MG132). MG132 was washed out, and cells were shifted to 30°C for 120 min. De novo synthesis of mCherry-VHL was inhibited by the addition of 10 µg/ml cycloheximide. Nuclei were visualized by coexpressing HTB1-cerulean (red). The dashed lines indicate the border of respective yeast cells. Bars, 1 µm. (C) Number (shaded bars) and localization (colored bars) of mCherry-VHL aggregates are shown in the respective strain at the indicated time points. The total number of foci per cell is depicted in all diagrams on the x axis. Quantifications are based on the analysis of 60–80 cells and are representatives of multiple experimental repeats.

mCherry-VHL foci, suggesting faster disaggregation (Fig. 6, B and C). Similar findings were obtained when stress-induced Hsp104-mCFP foci (37°C, +MG132, 180 min) were followed in WT and hsp42Δ cells upon return to physiological growth conditions, indicating a faster disintegration of endogenous protein aggregates in hsp42Δ cells (unpublished data). Foci disintegration is linked to Hsp104-mediated protein disaggregation, as clearance of juxtanuclear and peripheral mCherry-VHL foci was no longer observed in hsp104Δ cells (Fig. 6 B). Accordingly, hsp104Δ cells also showed a less pronounced reduction of mCherry-VHL foci upon prolonged incubation at 37°C (Fig. S3).

## Aggregate sequestration depends on an intact actin cytoskeleton

Next, we sought to determine whether the cytoskeleton plays a role in sequestering misfolded proteins to the juxtanuclear and peripheral compartments. The microtubule-depolymerizing drug benomyl has been shown to reversibly inhibit the formation of JUNQ and IPOD compartments, suggesting a crucial role of the microtubule cytoskeleton in aggregate sequestration (Kaganovich et al., 2008). We confirmed this observation but extended the analysis by including a benomyl-resistant yeast strain containing a mutation in tubulin-2 (Yang et al., 1997), which prevents benomyl from depolymerizing microtubules,

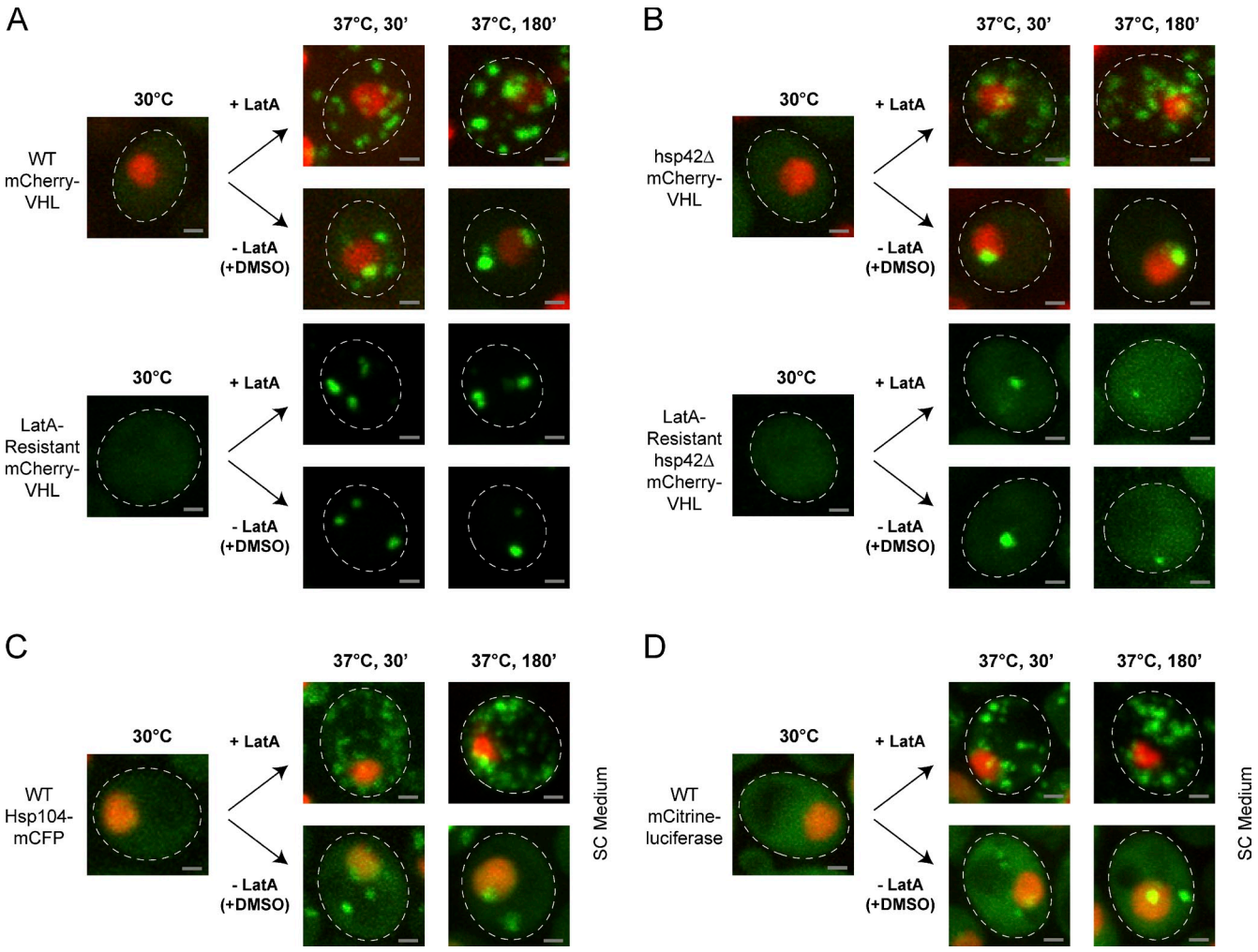


Figure 7. **The actin cytoskeleton is required for aggregate compartmentalization.** Reduction of mCherry-VHL (green) foci numbers during prolonged protein folding stress requires actin polymerization. Cells expressing mCherry-VHL were grown at 30°C and shifted to 37°C (+MG132). LatA or the same volume of DMSO as a control was added to the cells before a temperature shift. (A) mCherry-VHL localization was monitored in WT cells and cells containing a mutation in actin-1, which renders the actin cytoskeleton resistant to LatA. (B–D) hsp42Δ cells with or without the actin-1 mutation expressing mCherry-VHL (B) and WT cells expressing Hsp104-mCFP (C) or mCitrine-luciferase (D) were treated as described in A. All fluorescent reporter proteins are shown in green, and nuclei were visualized by coexpressing HTB1-cerulean (red). SC, synthetic complete. The dashed lines indicate the border of respective yeast cells. Bars, 1 µm.

to exclude secondary effects of the drug (Fig. S4). Similar to WT cells, the benomyl-resistant mutant cells did not form juxtanuclear and peripheral aggregates of mCherry-VHL at 37° upon treatment with benomyl. Instead, they contained multiple dispersed mCherry-VHL foci in the presence of benomyl after 30 and 180 min of incubation at 37°C. This demonstrates that the inhibitory effect of benomyl is microtubule independent, thereby questioning the role of microtubules in aggregate sequestration.

In *S. cerevisiae*, the actin cytoskeleton plays a dominant role in transport processes and has been recently linked to the asymmetric distribution of damaged proteins between yeast mother and daughter cells (Liu et al., 2010). Therefore, we determined whether sequestration of mCherry-VHL into juxtanuclear and peripheral aggregates requires an intact actin cytoskeleton. For this purpose, we monitored mCherry-VHL misfolding in the presence of the actin-depolymerizing drug latrunculin A (LatA), which causes complete disruption of the yeast actin cytoskeleton (Ayscough et al., 1997). After a 30-min incubation at 37°C, the LatA-treated cells displayed a vastly increased number of aggregates dispersed throughout the cytosol in contrast to DMSO-treated control cells (Fig. 7 A). Longer incubation (180 min) at 37°C did not result in a reduction of foci number in LatA-treated cells. As this is similar to our findings with benomyl that LatA could possibly have actin-independent secondary effects, we used a yeast strain containing a mutation in actin-1, which prevents LatA-mediated disassembly of the actin cytoskeleton (Ayscough et al., 1997). The LatA-resistant strain efficiently partitioned misfolded mCherry-VHL into juxtanuclear and peripheral compartments in the presence of LatA, reminiscent of untreated WT cells (Fig. 7 A). Importantly, LatA treatment did not reduce cell viability at the conditions tested (Fig. S5 A). The inhibitory effect of LatA on aggregate sorting is therefore directly linked to a nonfunctional actin cytoskeleton. The exclusive formation of juxtanuclear aggregates in hsp42Δ cells was also strictly dependent on an intact actin cytoskeleton, as LatA prevented juxtanuclear accumulation of mCherry-VHL

at 37°C in LatA-sensitive, but not resistant, cells (Fig. 7 B). Furthermore, the sorting of Hsp104-mCFP and mCitrine-luciferase aggregates into peripheral and juxtanuclear deposition sites was inhibited in the presence of LatA (Fig. 7, C and D). Therefore, a functional actin cytoskeleton plays a crucial, direct, or indirect role in aggregate partitioning in yeast cells.

## Discussion

In this study, we present an analysis of the initial formation and subsequent sequestration of protein aggregates into deposition sites in yeast cells subjected to sublethal protein folding stress. In accordance with previous findings (Kaganovich et al., 2008), we observed a partitioning of different fluorescent aggregation reporters between juxtanuclear and peripheral deposition sites. However, we found that the population of yeast cells subjected to stress exhibits significant heterogeneity with regard to the number of juxtanuclear and peripheral foci per cell. After application of extended protein folding stress (180 min at 37°C in the presence of MG132), only 50% of the cells has one juxtanuclear and one peripheral focus per cell, as reported earlier (Kaganovich et al., 2008), whereas the other 50% has more and sometimes even less foci of each kind. The relative prevalence of juxtanuclear foci increases with time during recovery. We interpret our findings as indicating that juxtanuclear and peripheral aggregates are not single distinct compartments within a yeast cell to which all aggregates are transported. Instead, we envision that the juxtanuclear and peripheral locations reflect different states of the aggregates, which allow association with distinct cellular structures such as the nuclear envelope or the perinuclear membrane in the case of juxtanuclear aggregates. Dependent on the applied stress conditions, such aggregates may form and be deposited until eliminated at one or several spots on these target structures. Notably, severe heat stress conditions (e.g., 45°C) strongly increased the number of dispersed foci in the case of all aggregation reporters, and, even after recovery for 2 h at 30°C, an increased number of peripheral mCherry-VHL aggregates relative to mild stress conditions was still present (unpublished data). Overall, our data show that the pattern of protein aggregation and hence the definition of the JUNQ and IPOD compartments is more complex than previously envisioned. Importantly, our data do not exclude the possibility that out of the ensemble of peripheral aggregates, only some are IPOD like, whereas others are functionally and physically distinct and even related to juxtanuclear aggregates.

The JUNQ and IPOD aggregates have been suggested to fulfill different cellular functions (Kaganovich et al., 2008). Juxtanuclear aggregates were reported to predominantly harbor ubiquitinated substrates, potentially allowing for their rapid elimination by the proteasome (Kaganovich et al., 2008). In contrast, peripheral aggregates are proposed to accumulate terminally misfolded and aggregated proteins, potentially protecting the cell from toxic protein species or facilitating aggregate clearance by either autophagy or dilution via cell division. Accordingly, mCherry-VHL molecules present in the juxtanuclear aggregates are more mobile compared with those sequestered at peripheral sites (Fig. 6 A; Kaganovich et al., 2008). On the other hand, we found that Hsp104 binds to both juxtanuclear and peripheral aggregates (Fig. 1 A), and the return of yeast cells to physiological growth conditions allowed for Hsp104-dependent disintegration of both types of aggregates (Fig. 6 B). The deposition of misfolded proteins at peripheral sites is therefore not an irreversible event, and the distribution between juxtanuclear and peripheral aggregates is not simply based on the decision whether a substrate can be refolded or not.

Our initial approach led to the identification of Hsp42 as an essential cellular factor in the formation of peripheral aggregates during physiological stress. Under the applied nonlethal stress conditions, misfolded endogenous yeast proteins and reporter proteins such as mCherry-VHL accumulate in hsp42Δ cells almost exclusively at the juxtanuclear site. Further, Hsp42 exerts a unique function in the formation of peripheral aggregates, as the other sHSP of yeast, Hsp26, did not affect aggregate sorting. Our finding that Hsp42 preferentially associates with peripheral foci suggests that this chaperone is directly involved in the targeting of aggregation-prone proteins to these sites. However, our data do not exclude the possibility that under some conditions, peripheral aggregates may also form independently of Hsp42. One such condition appears to be the formation of amyloidogenic protein aggregates, as indicated by the Hsp42-independent peripheral aggregation of RNQ1-YFP. Furthermore, a severe heat treatment at 45°C, which ultimately results in cell death, was found to alter the aggregation process, as significantly more peripheral aggregates were formed (Fig. 3 B) even in hsp42Δ cells. We assume that the 45°C heat shock treatment generates such high levels of misfolded proteins that the regular cellular sorting system becomes overwhelmed.

The selective absence of Hsp42 from the juxtanuclear aggregates provides a molecular criterion for the existence of two distinct forms of cytosolic protein aggregates. It is currently not evident which parameters prevent Hsp42 association with the juxtanuclear aggregates. One candidate is the ubiquitination status of the substrate, which has been previously shown to play a crucial role in targeting misfolded protein species to juxtanuclear inclusions and might interfere with Hsp42 association (Kaganovich et al., 2008).

The physiological consequences of redirecting misfolded proteins exclusively to the juxtanuclear site in hsp42Δ cells are not evident. We were surprised to note that juxtanuclear foci of hsp42Δ cells showed a moderate increase in substrate mobility and were slightly more rapidly solubilized by Hsp104. One interpretation of these results is that the Hsp42-dependent sorting to peripheral compartments retards substrate solubilization, thereby reducing substrate load for the quality control system. However, because hsp42Δ cells do not exhibit an apparent growth, stress sensitivity, or replicative ageing phenotype (unpublished data), the consequences of changing the flux of substrates into distinct compartments remain enigmatic.

Why does Hsp42 but not Hsp26 control aggregate sorting? Hsp26 requires increased temperature for activation, restricting its chaperone activity to heat stress conditions (Haslbeck et al., 1999; Franzmann et al., 2008). In contrast, Hsp42 appears to be constitutively active, allowing it to associate with misfolded proteins generated upon folding stress conditions distinct from

heat shock (Fig. 8; Haslbeck et al., 2004). Furthermore, we identified the large NTD of Hsp42 as a key determinant in contributing functional specificity to the sHSP. A ΔN-Hsp42 variant did not allow for the formation of peripheral inclusions. Conversely, the expression of an Hsp26 chimera, which has its NTD replaced by the Hsp42 NTD, partially restored the formation of peripheral inclusions in hsp42Δ mutant cells. NTDs of sHSPs have been demonstrated to mediate substrate interaction and sHSP oligomerization (Stromer et al., 2004; Basha et al., 2006; Jaya et al., 2009). Interestingly, a role of NTDs beyond their contribution to the chaperone activity of sHSPs has been noticed for Hsp16.6 from the cyanobacterium *Synechocystis*. Hsp16.6 N-terminal mutants possessed full chaperone functionality in vitro but displayed reduced ability to provide thermotolerance in vivo (Giese et al., 2005). Our findings indicate a function of the Hsp42 NTD in controlling the distribution of aggregated proteins between distinct deposition sites. We speculate that the elongated Hsp42 NTD remains partially exposed at the surface of the Hsp42 complexes with protein aggregates. Such a scenario implies the existence of further, so far unknown sorting factors that might bind to the Hsp42 NTD, thereby potentially directing protein aggregates to peripheral sites. This process may also involve the actin cytoskeleton, as its disruption in the presence of LatA abrogates aggregate sorting (Fig. 7). Although the effect of LatA was shown to be a direct one, we currently cannot exclude an indirect effect of actin cytoskeleton disruption on aggregate sorting, as the disintegration of the actin cytoskeleton also affects multiple transport processes and the cellular architecture. We considered the possibility that Hsp42 exerts an indirect effect by stabilizing the actin cytoskeleton during stress conditions (Gu et al., 1997). However, we did not observe differences in the organization of the actin cytoskeleton in hsp42Δ cells when compared with WT cells at both physiological and protein folding stress conditions (Fig. S5 B). Along the same lines, formation of the juxtanuclear aggregates was still observed in hsp42Δ cells but no longer upon disruption of the actin cytoskeleton by addition of LatA (Fig. 7), largely excluding the possibility that Hsp42 exerts its role by simply stabilizing the actin cytoskeleton.

In summary, we have identified a novel function for an sHSP in controlling the cellular sorting of damaged proteins (Fig. 8). In mammalian cells, K63-linked polyubiquitination of substrates is thought to serve as a signal for aggregate sorting by mediating the binding of the adaptor protein HDAC6, which links the ubiquitinated substrate to the microtubule motor protein dynein (Kawaguchi et al., 2003; Olzmann and Chin, 2008). The role of Hsp42 as a specific sorting label for protein inclusions represents a novel strategy. It is unclear whether this novel role of sHSPs in controlling the cellular localization of aggregated proteins is evolutionary conserved. Mammalian cells have been reported to sequester misfolded proteins into two distinct compartments like yeast cells (Kaganovich et al., 2008). However, Hsp42 homologues are only present in closely related fungi, suggesting that Hsp42 function might have been taken over by other members of the sHSP family. Intriguingly, the number of sHSP family members is strongly increased in higher eukaryotes (Haslbeck et al., 2005a), and sHSP function is no longer restricted to protein folding stress but is also linked to, for example, developmental processes and regulation of apoptosis (Arrigo, 2000; Heikkila, 2004). The evolutionary variability of N- and C-terminal extensions might enable sHSPs to adopt novel functions, including the cellular sorting of aggregated proteins, thereby potentially taking over the function of Hsp42 in yeast.

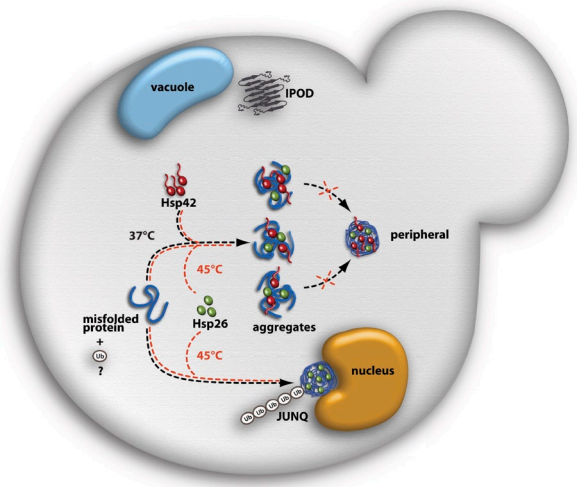


Figure 8. **Model depicting the roles of Hsp42 and Hsp26 in aggregate sorting in yeast cells experiencing sublethal folding stress.** Hsp42 exclusively associates with peripheral protein aggregates during physiological folding stress (37°C) but is absent from juxtanuclear aggregates (JUNQ). The formation of peripheral foci depends on the elongated NTD of Hsp42. Hsp26 is absent from protein aggregates at 37°C but associates with peripheral and juxtanuclear aggregates during lethal heat stress (45°C). Hsp42 does not associate with the IPOD compartment harboring amyloidogenic proteins close to the vacuole. Ubiquitination (Ub) might serve as a sorting signal for juxtanuclear aggregates.

## Materials and methods

### Yeast media, strains, and plasmids

Yeast media preparation, growth, and transformations as well as recombinant DNA methods were performed as previously described (Maniatis et al., 1989; Abelson et al., 2003). All genes were cloned by PCR from yeast genomic DNA or a template plasmid and verified by sequencing. Chromosomal mCFP and mCitrine tagging was performed using the optimized cassettes for fluorescent protein tagging in *S. cerevisiae* (Sheff and Thorn, 2004). The genotypes of the plasmids and strains used in this study are summarized in Tables S1 and S2, respectively.

### Inhibitor treatment

Cells were grown until midlog phase ($OD_{600}$ = 0.5) at 30°C. For experiments using MG132, BY4741 strains lacking the Pdr5 transporter were used as WT. Deletion of Pdr5 sensitizes cells to the proteasome inhibitor. Before a temperature shift to 37°C, MG132 dissolved in DMSO was added to a final concentration of 80 µM. Where indicated, LatA or benomyl dissolved in DMSO was added before a temperature shift to 37°C to a final concentration of 200 µM or 20 µg/ml, respectively. The same amount of DMSO was added to the control. To monitor the stability of juxtanuclear and peripheral compartments, cells were incubated at 37°C for 180 min (+MG132). Subsequently, cells were washed, and the translation inhibitor cycloheximide dissolved in ethanol was added to a final concentration of 10 µg/ml before starting the recovery at 30°C. The same amount of ethanol was added to the control. For all experiments, VHL expression was shut off before temperature shift and microscopy by addition of 2% glucose.

### Viability assays

For thermotolerance analysis, overnight cultures of yeast cells were diluted into fresh yeast peptone dextrose (YPD) medium and grown to midlog phase.

Cells were first shifted to 37°C for 60 min and then incubated at 50°C for the indicated period of time. Samples were taken, serially diluted fivefold, and spotted onto YPD plates, and survival of cells was determined by calculating the plating efficiency after 2 d of growth at 30°C. For viability analysis in response to LatA, cells were grown until midlog phase at 30°C. Before a temperature shift to 37°C, MG132 and LatA were added to a final concentration of 80 µm or 200 µM, respectively. The same amount of DMSO was added to the control. After incubation for 180 min at 37°C, cells were washed and spotted onto agar plates as described for thermotolerance analysis.

**FLIP analysis**

For FLIP analysis, cells were grown to midlog phase, immobilized on concanavalin A–coated glass-bottom culture dishes, and incubated at 37°C for 180 min (+MG132) before FLIP measurements were started. 25 individual cells each for the WT and hsp42Δ strains were measured. A small section of cytosolic fluorescence outside of the inclusions was bleached in 30 cycles of acquisition (0.5 s, 1–2% laser intensity) and bleach (0.49 s, 100% laser intensity). Measurements were performed at 37°C on a laser-scanning confocal microscope (A1R; Nikon). The resulting loss of fluorescence in the region of interest as a function of time provides a measure of the relative exchange rate with the bleached cytoplasmic fraction of molecules.

**Immunofluorescence**

Cells were fixed and stained as previously described (Gavin, 2009). In short, cells were fixed with 4% PFA at the growth temperature and subsequently digested with Zymolyase 100T to remove the cell wall. Spheroblasts were permeabilized with 1% Triton X-100 in PBS and blocked with 1% BSA in PBS before antibody staining. Incubation with anti-Hsp42 (1:400 dilution; provided by M. Haslbeck and J. Buchner, Technische Universität München Institut für Organische Chemie und Biochemie, Garching, Germany; Haslbeck et al., 2004), anti-Hsp26 (1:100 dilution), and anti-FLAG (1:500) was performed for 2 h at room temperature. The secondary antibody (Alexa Fluor 488 $F(ab')_2$ fragment of goat anti–rabbit IgG) was diluted 1:1,000, and incubation was performed for 1 h at room temperature. When indicated, 100 ng/ml DAPI was included at the secondary antibody incubation for visualization of the nucleus.

**Image acquisition, processing, and data analysis**

Confocal micrographs were obtained from living yeast cells on a spinning-disk microscope with a 100× oil lens (NA 1.4). 12-bit digital images were acquired with a cooled charge-coupled device camera and processed by using ImageJ (National Institutes of Health) and Photoshop (Adobe) software. For snapshot imaging, cells were recovered by centrifugation, washed in PBS, and immobilized on agarose pads. To avoid dehydration, the agarose pads were sealed with Apiezon grease and covered with coverslips. For time-lapse imaging, cells were immobilized on concanavalin A–coated coverslips, immersed in medium, and sealed in a custom-made aluminum slide using coverslips on each side. The slide was subsequently placed into a custom-made metal holder that was connected to a Peltier element, which allowed accurate temperature control. Image processing was performed using ImageJ and Photoshop software. Statistics of aggregation foci number and localization and plotting of the data were performed with Excel (Microsoft) and KaleidaGraph (Synergy Software) software. The number of cells analyzed is indicated in the figure legends.

**Online supplemental material**

Fig. S1 shows that *S. cerevisiae* Hsp104-mCFP provides WT-like thermotolerance. Fig. S2 shows that the NTD of Hsp42 mediates sorting of aggregated proteins to peripheral inclusions. Fig. S3 shows formation of mCherry-VHL foci in hsp104Δ cells. Fig. S4 shows that microtubule-independent effects of benomyl prevent aggregate sorting of misfolded mCherry-VHL into JUNQ and IPOD-like compartments. Fig. S5 shows that LatA treatment does not reduce cell viability, and the actin cytoskeleton is not altered in hsp42Δ cells at both physiological and folding stress conditions. Tables S1 and S2 show plasmids and *S. cerevisiae* strains, respectively, used in this study. Online supplemental material is available at http://www.jcb.org/cgi/content/full/jcb.201106037/DC1.

We thank E. Schiebel and J. Tyedmers for discussion and inspiring ideas, U. Engel and C. Ackermann (Nikon Imaging Center at the University of Heidelberg) and H. Lorenz (Zentrum für Molekulare Biologie der Universität Heidelberg imaging facility) for support in microscopy and data analysis, and L. Guilbride for editing of the manuscript. We are grateful to J. Buchner and M. Haslbeck for providing Hsp26- and Hsp42-specific antibodies, K.R. Ayscough for strains KAY0159 and KAY0173, and J. Frydman for plasmid pESC-mCherry-VHL.

S. Specht was supported by a fellowship of the Fonds der Chemischen Industrie. S.B.M. Miller was supported by a fellowship of the Boehringer Ingelheim Fonds and by the Hartmut Hoffmann-Berling International Graduate School of Molecular and Cellular Biology. This work received support from the Network for Aging Research of the University of Heidelberg.

Submitted: 6 June 2011
Accepted: 13 October 2011

## References

Abelson, J.N., C. Guthrie, and G.R. Fink. 2003. Guide to Yeast Genetics and Molecular Biology. Academic Press, New York. 933 pp.

Arrigo, A.P. 2000. sHsp as novel regulators of programmed cell death and tumorigenicity. *Pathol. Biol. (Paris)*. 48:280–288.

Ayscough, K.R., J. Stryker, N. Pokala, M. Sanders, P. Crews, and D.G. Drubin. 1997. High rates of actin filament turnover in budding yeast and roles for actin in establishment and maintenance of cell polarity revealed using the actin inhibitor latrunculin-A. *J. Cell Biol.* 137:399–416. http://dx.doi.org/10.1083/jcb.137.2.399

Basha, E., K.L. Friedrich, and E. Vierling. 2006. The N-terminal arm of small heat shock proteins is important for both chaperone activity and substrate specificity. *J. Biol. Chem.* 281:39943–39952. http://dx.doi.org/10.1074/jbc.M607677200

Cashikar, A.G., M. Duennwald, and S.L. Lindquist. 2005. A chaperone pathway in protein disaggregation. Hsp26 alters the nature of protein aggregates to facilitate reactivation by Hsp104. *J. Biol. Chem.* 280:23869–23875. http://dx.doi.org/10.1074/jbc.M502854200

Franzmann, T.M., P. Menhorn, S. Walter, and J. Buchner. 2008. Activation of the chaperone Hsp26 is controlled by the rearrangement of its thermosensor domain. *Mol. Cell*. 29:207–216. http://dx.doi.org/10.1016/j.molcel.2007.11.025

García-Mata, R., Z. Bebök, E.J. Sorscher, and E.S. Sztul. 1999. Characterization and dynamics of aggresome formation by a cytosolic GFP-chimera. *J. Cell Biol.* 146:1239–1254. http://dx.doi.org/10.1083/jcb.146.6.1239

Gavin, R.H. 2009. Cytoskeleton Methods and Protocols, Second edition. Humana Press, New York. 388 pp.

Giese, K.C., and E. Vierling. 2002. Changes in oligomerization are essential for the chaperone activity of a small heat shock protein in vivo and in vitro. *J. Biol. Chem.* 277:46310–46318. http://dx.doi.org/10.1074/jbc.M208926200

Giese, K.C., E. Basha, B.Y. Catague, and E. Vierling. 2005. Evidence for an essential function of the N terminus of a small heat shock protein in vivo, independent of in vitro chaperone activity. *Proc. Natl. Acad. Sci. USA*. 102:18896–18901. http://dx.doi.org/10.1073/pnas.0506169103

Gu, J., M. Emerman, and S. Sandmeyer. 1997. Small heat shock protein suppression of Vpr-induced cytoskeletal defects in budding yeast. *Mol. Cell. Biol.* 17:4033–4042.

Haslbeck, M., S. Walke, T. Stromer, M. Ehrnsperger, H.E. White, S. Chen, H.R. Saibil, and J. Buchner. 1999. Hsp26: A temperature-regulated chaperone. *EMBO J.* 18:6744–6751. http://dx.doi.org/10.1093/emboj/18.23.6744

Haslbeck, M., N. Braun, T. Stromer, B. Richter, N. Model, S. Weinkauf, and J. Buchner. 2004. Hsp42 is the general small heat shock protein in the cytosol of *Saccharomyces cerevisiae*. *EMBO J.* 23:638–649. http://dx.doi.org/10.1038/sj.emboj.7600080

Haslbeck, M., T. Franzmann, D. Weinfurtner, and J. Buchner. 2005a. Some like it hot: The structure and function of small heat-shock proteins. *Nat. Struct. Mol. Biol.* 12:842–846. http://dx.doi.org/10.1038/nsmb993

Haslbeck, M., A. Miess, T. Stromer, S. Walter, and J. Buchner. 2005b. Disassembling protein aggregates in the yeast cytosol. The cooperation of Hsp26 with Ssa1 and Hsp104. *J. Biol. Chem.* 280:23861–23868. http://dx.doi.org/10.1074/jbc.M502697200

Heikkila, J.J. 2004. Regulation and function of small heat shock protein genes during amphibian development. *J. Cell. Biochem.* 93:672–680. http://dx.doi.org/10.1002/jcb.20237

Jaya, N., V. Garcia, and E. Vierling. 2009. Substrate binding site flexibility of the small heat shock protein molecular chaperones. *Proc. Natl. Acad. Sci. USA*. 106:15604–15609. http://dx.doi.org/10.1073/pnas.0902177106

Johnston, J.A., C.L. Ward, and R.R. Kopito. 1998. Aggresomes: A cellular response to misfolded proteins. *J. Cell Biol.* 143:1883–1898. http://dx.doi.org/10.1083/jcb.143.7.1883

Kaganovich, D., R. Kopito, and J. Frydman. 2008. Misfolded proteins partition between two distinct quality control compartments. *Nature*. 454:1088–1095. http://dx.doi.org/10.1038/nature07195

Kawaguchi, Y., J.J. Kovacs, A. McLaurin, J.M. Vance, A. Ito, and T.P. Yao. 2003. The deacetylase HDAC6 regulates aggresome formation and cell

viability in response to misfolded protein stress. *Cell*. 115:727–738. http://dx.doi.org/10.1016/S0092-8674(03)00939-5

Lelouard, H., E. Gatti, F. Cappello, O. Gresser, V. Camosseto, and P. Pierre. 2002. Transient aggregation of ubiquitinated proteins during dendritic cell maturation. *Nature*. 417:177–182. http://dx.doi.org/10.1038/417177a

Lindner, A.B., R. Madden, A. Demarez, E.J. Stewart, and F. Taddei. 2008. Asymmetric segregation of protein aggregates is associated with cellular aging and rejuvenation. *Proc. Natl. Acad. Sci. USA*. 105:3076–3081. http://dx.doi.org/10.1073/pnas.0708931105

Liu, B., L. Larsson, A. Caballero, X. Hao, D. Oling, J. Grantham, and T. Nyström. 2010. The polarisome is required for segregation and retrograde transport of protein aggregates. *Cell*. 140:257–267. http://dx.doi.org/10.1016/j.cell.2009.12.031

Maniatis, T., J. Sambrook, and E.F. Fritsch. 1989. Molecular Cloning: A Laboratory Manual. Second edition. Cold Spring Harbor Laboratory Press, Cold Spring Harbor, NY. 1659 pp.

McClellan, A.J., M.D. Scott, and J. Frydman. 2005. Folding and quality control of the VHL tumor suppressor proceed through distinct chaperone pathways. *Cell*. 121:739–748. http://dx.doi.org/10.1016/j.cell.2005.03.024

Mogk, A., E. Deuerling, S. Vorderwülbecke, E. Vierling, and B. Bukau. 2003. Small heat shock proteins, ClpB and the DnaK system form a functional triade in reversing protein aggregation. *Mol. Microbiol.* 50:585–595. http://dx.doi.org/10.1046/j.1365-2958.2003.03710.x

Morimoto, R.I. 2008. Proteotoxic stress and inducible chaperone networks in neurodegenerative disease and aging. *Genes Dev*. 22:1427–1438. http://dx.doi.org/10.1101/gad.1657108

Olzmann, J.A., and L.S. Chin. 2008. Parkin-mediated K63-linked polyubiquitination: A signal for targeting misfolded proteins to the aggresome-autophagy pathway. *Autophagy*. 4:85–87.

Ratajczak, E., S. Zietkiewicz, and K. Liberek. 2009. Distinct activities of *Escherichia coli* small heat shock proteins IbpA and IbpB promote efficient protein disaggregation. *J. Mol. Biol.* 386:178–189. http://dx.doi.org/10.1016/j.jmb.2008.12.009

Rizzo, M.A., G.H. Springer, B. Granada, and D.W. Piston. 2004. An improved cyan fluorescent protein variant useful for FRET. *Nat. Biotechnol.* 22:445–449. http://dx.doi.org/10.1038/nbt945

Rokney, A., M. Shagan, M. Kessel, Y. Smith, I. Rosenshine, and A.B. Oppenheim. 2009. *E. coli* transports aggregated proteins to the poles by a specific and energy-dependent process. *J. Mol. Biol.* 392:589–601. http://dx.doi.org/10.1016/j.jmb.2009.07.009

Rujano, M.A., F. Bosveld, F.A. Salomons, F. Dijk, M.A. van Waarde, J.J. van der Want, R.A. de Vos, E.R. Brunt, O.C. Sibon, and H.H. Kampinga. 2006. Polarised asymmetric inheritance of accumulated protein damage in higher eukaryotes. *PLoS Biol.* 4:e417. http://dx.doi.org/10.1371/journal.pbio.0040417

Schröder, H., T. Langer, F.-U. Hartl, and B. Bukau. 1993. DnaK, DnaJ and GrpE form a cellular chaperone machinery capable of repairing heat-induced protein damage. *EMBO J.* 12:4137–4144.

Sheff, M.A., and K.S. Thorn. 2004. Optimized cassettes for fluorescent protein tagging in *Saccharomyces cerevisiae*. *Yeast*. 21:661–670. http://dx.doi.org/10.1002/yea.1130

Stromer, T., E. Fischer, K. Richter, M. Haslbeck, and J. Buchner. 2004. Analysis of the regulation of the molecular chaperone Hsp26 by temperature-induced dissociation: The N-terminal domail is important for oligomer assembly and the binding of unfolding proteins. *J. Biol. Chem.* 279:11222–11228. http://dx.doi.org/10.1074/jbc.M310149200

Szeto, J., N.A. Kaniuk, V. Canadien, R. Nisman, N. Mizushima, T. Yoshimori, D.P. Bazett-Jones, and J.H. Brumell. 2006. ALIS are stress-induced protein storage compartments for substrates of the proteasome and autophagy. *Autophagy*. 2:189–199.

Winkler, J., A. Seybert, L. König, S. Pruggnaller, U. Haselmann, V. Sourjik, M. Weiss, A.S. Frangakis, A. Mogk, and B. Bukau. 2010. Quantitative and spatio-temporal features of protein aggregation in *Escherichia coli* and consequences on protein quality control and cellular ageing. *EMBO J.* 29:910–923. http://dx.doi.org/10.1038/emboj.2009.412

Yang, S., K.R. Ayscough, and D.G. Drubin. 1997. A role for the actin cytoskeleton of *Saccharomyces cerevisiae* in bipolar bud-site selection. *J. Cell Biol.* 136:111–123. http://dx.doi.org/10.1083/jcb.136.1.111